SUPPLEMENTAL FIGURE S1

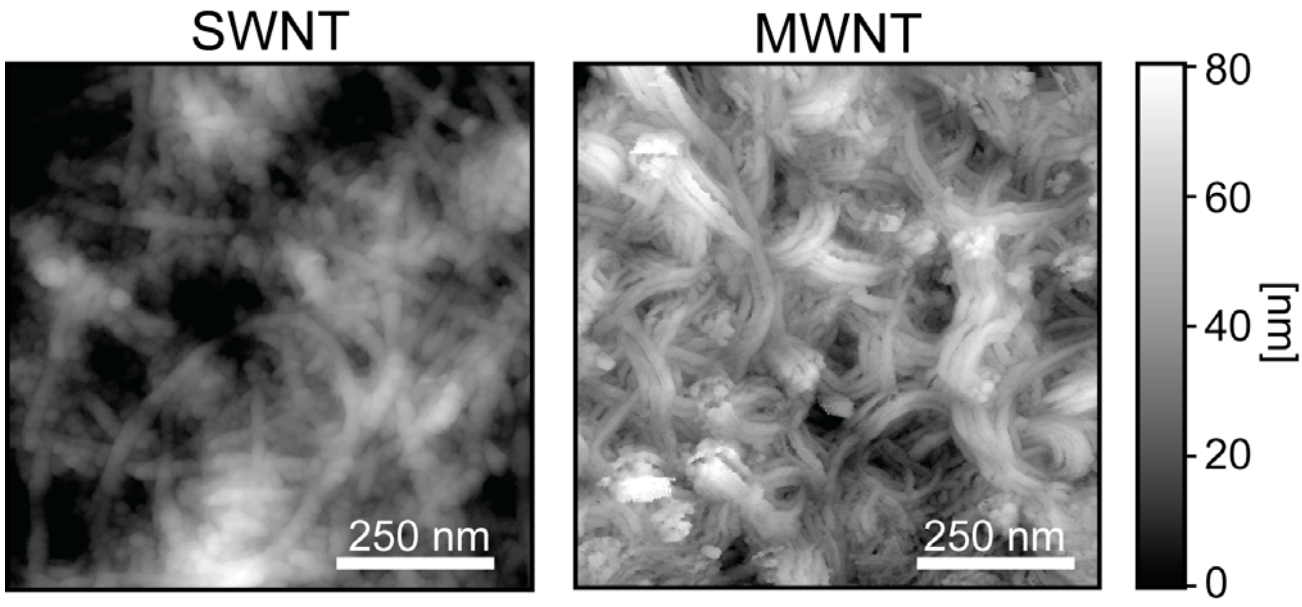

AFM imaging reveals the 3-dimensional nanomeshworks in nanotubes substrates, composed of single walled nanotubes (**left**) and of multi walled nanotubes (**right**).

SUPPLEMENTAL METHODS

Tissue cultures

Hippocampi were dissected from 0/3-d old Sprague Dawley rats killed by decapitation. This procedure is in accordance with the relevant EU legislation. Hippocampal slices were digested and cells were plated on peptide-free or on CNT treated glass coverslips and cultured for 8-14 days (Lovat et al, 2005). Dissociated DRG cultures (20 series) were prepared according to Fucile et al. (2005). DRG neurons were dissected from 1-4 days old Sprague Dawley rats, killed by decapitation. Thoracic and lumbar DRG were digested, and cells were plated on peptide free or MWNT coated glass coverslips and cultured for 8-14 days.

Electrophysiological recordings

Recording solution contained (mM): NaCl 150, KCl 4, $MgCl_2$ 1, $CaCl_2$ 2, HEPES 10, glucose 10, at room temperature, pH 7.4 adding NaOH (Mazzatenta *et al.*, 2007; Lovat *et al.*, 2005). All agents were bath-applied; these included 6-cyano-7-nitroquinoxaline-2,3-dione (CNQX, Sigma-Aldrich, Italy), gabazine (SR-95531, Sigma-Aldrich, Italy), nifedipine (Sigma-Aldrich, Italy), nickel chloride (AnalaR-BDH Chemical, England), cobalt chloride (C-3169, Sigma-Aldrich, Italy).

Whole-cell patch-clamp recordings were obtained at room temperature employing patch-pipettes (4-7 MΩ), under GΩ patch sealing, using an Axopatch 1-D (Axon Instruments, Foster City, CA, USA) or an EPC-7 amplifier (List, Germany) for voltage clamp recordings; for current clamp recordings (obtained in bridge mode after negative capacity compensation) were amplified by an Axoclamp 2 unit (Axon Instruments) and processed in the same way as those collected under voltage clamp conditions. Intracellular solution contained, for voltage clamp recordings, (mM): K gluconate 120, KCl 20, HEPES 10, EGTA 10, $MgCl_2$ 2 and Na_2ATP 2 (pH 7.35 adding KOH). Current clamp recordings used a similar solution where EGTA was omitted and compensated by 10 mM increase in K gluconate. In voltage-clamp holding potential was set at -58 mV. Values of membrane potentials were systematically corrected for liquid junction potentials and other offset potentials. The uncompensated value for series resistance was <8-10 MΩ. In current-clamp recordings, bridge balancing was continuously monitored and adjusted.

Responses were amplified and stored for further analysis, digitized at 10-20 kHz with the pCLAMP 9 software (Axon Instruments, Foster City, CA). Events which appeared as summated responses or were superimposed on a large event were discarded. Single spontaneous synaptic events were detected by use of the AxoGraph 3.5.5 (Axon Instruments) event detection software on a MacIntosh computer (Clements and Bekkers, 1997).

TEM and RADA16 AFM analysis

For TEM analysis, cultures (n=6 from 3 different culture series) after 8-10 days in vitro, were fixed with a solution containing 2.5% glutaraldehyde (Fluka, Italy) in 0.1 M cacodylate buffer, pH 7.4, for 1 h at RT. Cultures were then washed in cacodylate buffer for several times and then transferred into a PBS solution containing 1% osmium tetroxide (Fluka) for 1 h at RT. Cultures were then dehydrated in graded ethanol and embedded in epoxi resina (DER 332-732). Ultrathin sections (85 nm) were obtained from cultures, by cutting the samples in a planar and in a perpendicular plane to the surface. Sections (n=36) were then collected onto 300 mesh nickel grids, stained with uranyl acetate and lead citrate (Fluka) and examined with a Philips EM 208 by the digital acquisition system GATAN TVC 673. The morphological analysis was performed on digital images obtained from 50 randomly-selected grid-fields.

RADA16 slides preparation for AFM analysis is described elsewhere (Gelain *et al.*, 2007).

Statistical analysis

All electrophysiological values from batches of cultures subjected to the same experimental protocols were pooled together and expressed as mean ± s.d. with n=number of cells, when not otherwise stated. Statistical analysis was carried out using the Student's and Chi Square's tests ($p<0.05$). In addition, differences in the relative cumulative frequency distribution were obtained using the paired Kolmogorov–Smirnov test ($p<0.005$).

"Peeling" of the electrotonic membrane time constants

Under current clamp configuration and in the presence of CNQX and gabazine, a set of experiments was dedicated to the assessment of time constants in response to transient voltage response following step current pulse (-0.03 nA and 5 or 10 ms) injected at the soma (Holmes et al., 1992; Segev, 2006).

We compared DRG and hippocampal neurons grown on control substrates or on CNT. No difference in the represented values of τ_i in CNT-systems seems to emerge from the four groups of cells (see Supplemental Results).

Single-neuron model

Similar to the reduced model of Larkum *et al.* (2004), we defined and computer-simulated a two-compartmental Integrate-and-Fire neuron. The model is fully characterized by two state variables V_s and V_d, describing in effective terms the voltage distributions of a somatic and a dendritic compartment, respectively (Figure 4c). Variables evolve in time according to the following equations, which represent the balance of electrical charge (Figure 4d):

$$C_s \, dV_s / dt = g_s (E_s - V_s) + g_x (V_d - V_s) + I_{syn}$$
$$C_d \, dV_d / dt = g_d (E_d - V_d) + g_x (V_s - V_d),$$

where $C_{s/d}$, $g_{s/d}$, $E_{s/d}$ are the somatic (dendritic) membrane capacitance, conductance and reversal potential, respectively. As soon as the somatic voltage exceed a fixed threshold V_{th}, V_s is reset to V_{reset}, as in Integrate-and-Fire models (Abbott and Dayan, 2001), and V_d is instantaneously increased of $\Delta \, g_x / C_d$. This mimicks the total charge transferred to dendritic compartments by a backpropagating action-potential and mediated by dendritic voltage-gated calcium channels. Because V_d accumulates the contributions of closely fired somatic action potentials (e.g. see Figure 4e), it acts as a kind of 'charge reservoir', which discharges back to the somatic compartment. When somato-dendritic coupling is weak (i.e. $\Delta = \Delta_0 << 1$), the dendritic compartment experience almost no effect upon somatic spiking (Figure C, upper panel). On the contrary, when the dendrite is charged by somatic spikes (i.e. $\Delta = \Delta_+ >> 1$), the model neuron fires spontaneously with the same rate, although some firing epoch might be prolonged by the extra depolarization (i.e. ADP – Figure C, lower panels).

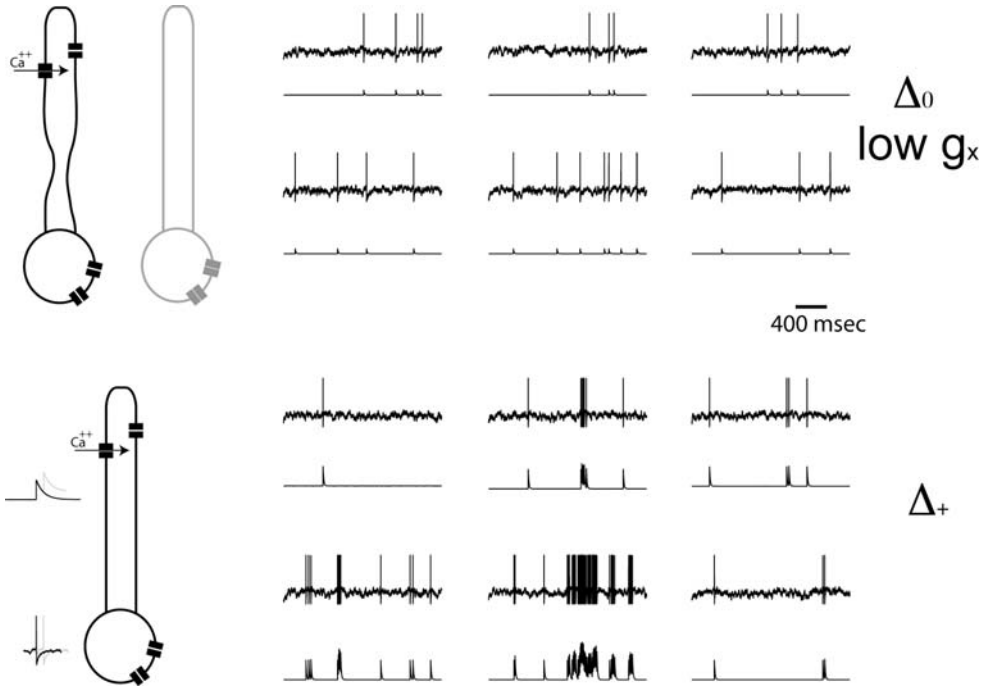

Fig C: Simulated firing of a single model neuron, whose parameters are chosen to represent (**upper panels**) weak somato-dendritic interactions, and (**lower panels**) strong somato-dendritic coupling. As intuitively expected, the extra depolarization (i.e. ADP - see Figure 4e) following a burst of closely fired somatic spikes may prolong neuronal firing, only when the somato-dendritic coupling is strong.

Model of an in vitro neuronal network

A homogeneous population of 50 randomly connected excitatory model neurons, defined as described in the previous section, was defined and computer simulated. This aims at representing the collective electrical activity in a small local neuronal population in a Petri dish. Although the impact of the CNT-substrate is simulated indirectly through the intrinsic parameter Δ, we used this model to predict network-level consequences (Lovat *et al.*, 2005) of the after-potential depolarization reported in this work.

Indicating with t_k, the times of emission of a spike by a presynaptic neuron, postsynaptic coupling was described by

$$I_{syn} = \sum_k J_{e\,k}\, C \exp[-(t-t_k)]\, \Theta(t-t_k)$$

where C is '1' only if the two neurons are connected, Θ(t) is the step function (i.e., $\Theta(t) = 0$, $t < 0$ and $\Theta(t) = 1$, $t > 0$). Short-term (homo)synaptic depression was included in the model as in Tsodyks *et al.*, (1998). Briefly, synaptic efficacy $J_{e\,k}$ at a generic k-*th* synapse was not constant in time, but decreased in amplitude spike (i.e. $J_e = J_e * u$, where $u < 1$) after each (presynaptic) spike that recruited that particular synapse. Thus, synaptic efficacy was dependent on the presynaptic inter-spike intervals (i.e. $t_k - t_{k-1}$), as it recovered exponentially to its resting value $J_{resting}$ between any two spikes ($J_{e\,k} = (J_{e\,k} - J_{resting}) \exp[-(t_k - t_{k-1}) / \tau_{rec}]$). Following the same considerations of Giugliano *et al.*, (2004), we chose an unstructured connection topology (Marom and Shahaf 2002) with a uniform pair-wise probability of synaptic connection between any two neurons of 0.3–0.4. The effect of spontaneous synaptic release and of other sources of randomness (Maeda *et al.* 1995) was incorporated into an activity-independent additional random synaptic drive.

As these networks were analyzed in terms of their mean-field description (see Giugliano et al., 2004; and Giugliano *et al.*, 2008 for a review) and showed to account for irregular population bursting, the model predictions and results described in the main text do not depend on the individual realizations of this network topology. In facts, such model network is able to generate episodes of synchronous spontaneous firing (Figure D; see also Tsodyks *et al.*, 2000), resembling the endogenous activity observed in cultured neurons (Lovat *et al.*, 2005; Giugliano *et al.*, 2004; Marom and Shahaf, 2002).

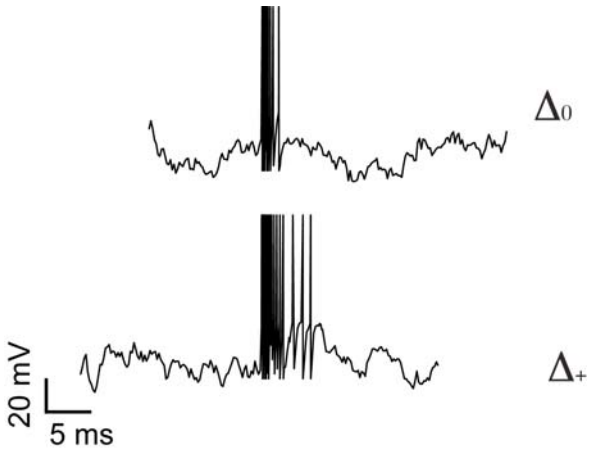

Fig D: Simulated firing of two neurons, embedded in a model network. When individual neuron parameters are chosen to describe (**upper panels**) weak somato-dendritic interactions, spontaneous irregular burst of action potentials (i.e. population bursts - PBs) occurs synchronously in the network. Similarly, (**lower panels**) for strong somato-dendritic coupling the probability of PB ignition remains largely unaffected but the duration of each event is prolonged.

Estimation of the average PSC event in the experiments

Long epochs of spontaneous activity, recorded under voltage-clamp obtained from 3 cultures growing on CNT and from 3 cultures growing on control glass, were analyzed. Raw-traces mostly represented the total membrane current due to synaptic inputs and any contribution from intrinsic voltage-gated currents was neglected. After de-trending each waveform, presynaptic events were extracted by a custom peak-detection algorithm, based on threshold-crossing. This procedure employed an adaptive threshold and a detection-refractoriness of 200 ms. The same detection parameters were employed in the analysis of both CNT and control groups. Individual extracted events (i.e. ~100 – 400 / recording) were aligned to the time of threshold crossing and averaged point-by-point, 50 ms before and 150 ms after. The resulting waveform relates to the probability of synaptic events clustering, within a window of [50 ms; 150 ms]. This operatively defines a burst of presynaptic action potentials. In all the experiments, synaptic events were composed of synchronized presynaptic firing, as apparent from their large amplitude (i.e. >~ 500 pA) compared to the typical miniature synaptic potential (93±4 pA, not shown).

SUPPLEMENTAL RESULTS

Time constants peeling

For the peeling of the membrane time constants, current-clamp recordings of subthreshold membrane voltage, evoked by brief hyperpolarizing current pulsed, were employed (D'Aguanno et al., 1986; Holmes et al., 1986). Voltage transients were first normalized to values between 0 (i.e. resting level) and 1 (i.e. the value immediately after the pulse) and then fit to a sum of 6

exponentials as $W(t) = C_1 \exp(-t / \tau_1) + \ldots + C_6 \exp(-t / \tau_6)$. The values of $\{ C_i , \tau_i \}$ were chosen through an optimization procedure, based on simulated annealing and implemented in Matlab (The Mathworks, Natick, US).

Time constants peeling for electrotonic length estimates

We identified best-fit parameters of a superposition of 6 exponentials, to match experimental transient voltage responses, recorded somatically in hippocampal as well as in spinal DRG cultured neurons. The accuracy of the fit was well below 0.03%, corresponding to a mean square error of about few hundreds of μV. Typical examples of the traces and their fit profiles are reported in Fig A

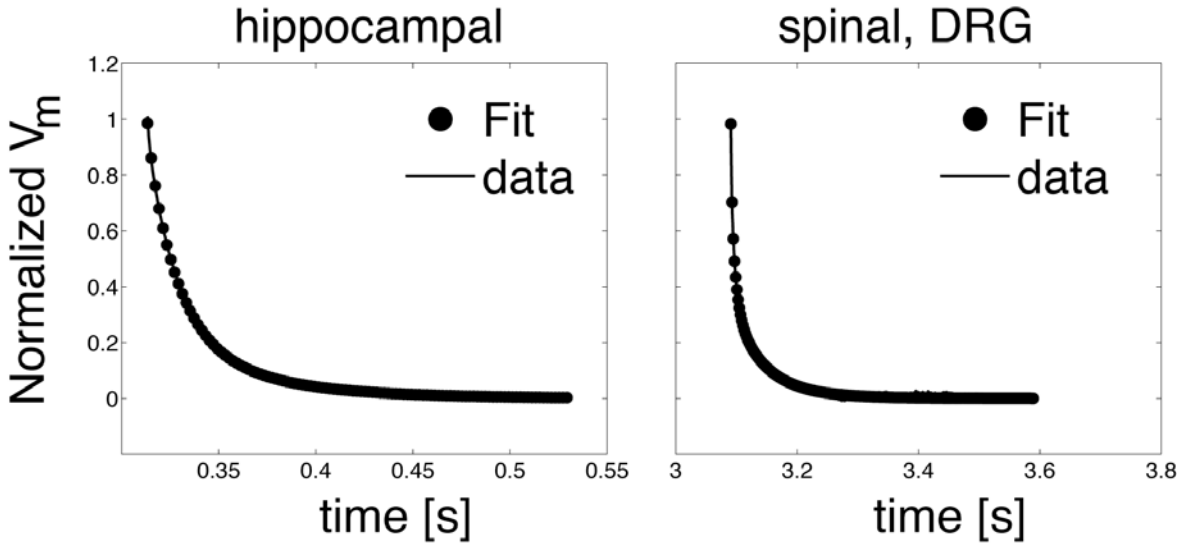

Fig A: Sample normalized voltage transients recorded somatically in cultured neurons, dissociated from the hippocampus (**left**) and from the spinal cord (**DRG – right**). Markers represent the best-fit predictions of the multi-exponential function, as indicated in the text.

Although inferring cable passive properties through exponential peeling of voltage transients requires great care for complex branched morphologies (Holmes et al., 1992), here we tested the impact of CNT growth substrates on the electrotonic membrane properties of cultured neurons. We specifically searched for differences in CNT-neuronal interactions between arborized- (i.e. hippocampal cells) and non arborized-morphologies (i.e. DRG neurons), compared to respective control conditions.

No significant differences in the distributions of best-fit (peeled) time-constants were observed, within each of the two groups: hippocampal neurons with/without CNT (Fig. B, left), DRG neurons with/without CNT (Fig. B, right). This result suggests that the enhanced, CNT-mediated, somato-dendritic coupling requires an active, and not passive, extracellular "short-cut" between the different neuronal compartments.

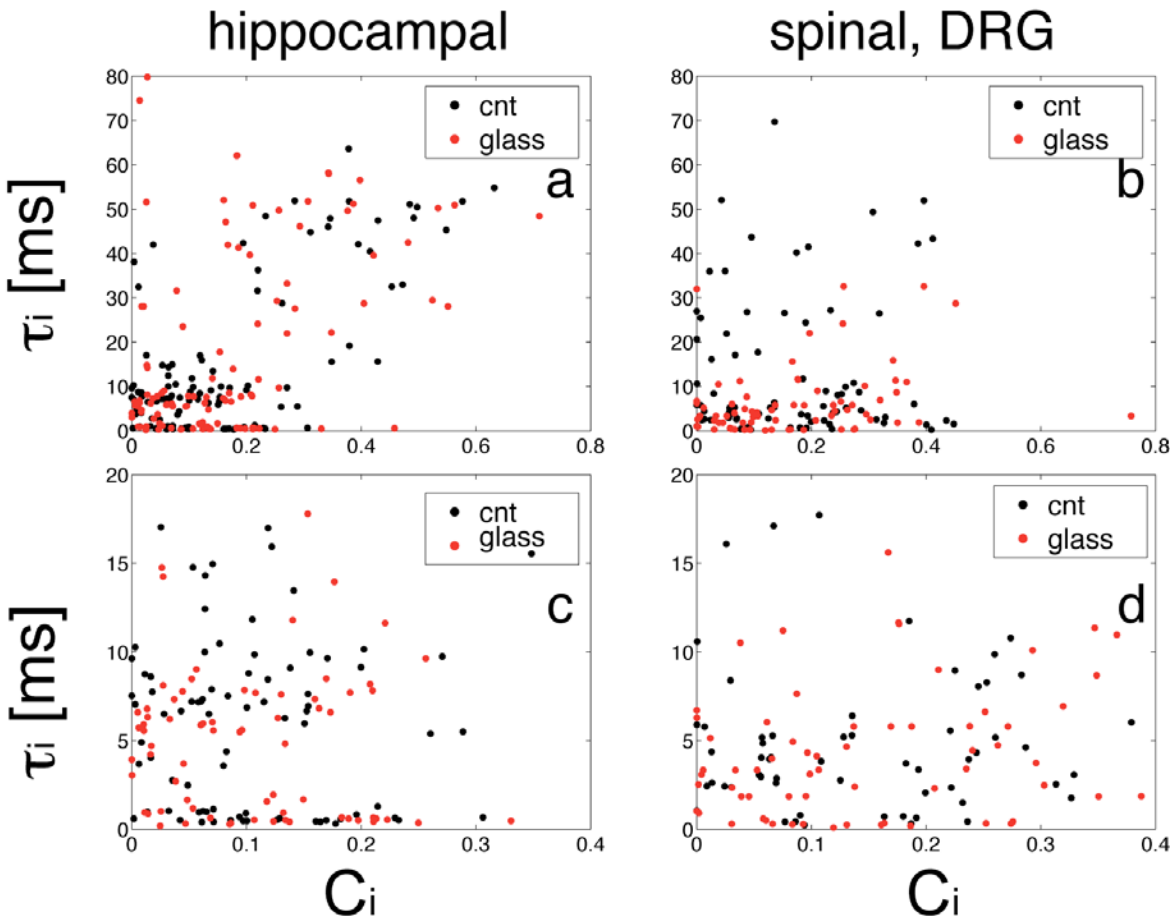

Fig. B: Scatter plot (and its zoomed details, bottom panels) of the couples (C_i, τ_i) best fitting the exponential transient in the data recorded in hippocampal neurons (**a – c**) and DRG neurons (**b – d**). No difference in the represented values of τ_i seems to emerge within the two groups of cells. Note that the very small time constant matched by a large C_i corresponds to the filtering impact of the pipette.

SUPPLEMENTAL REFERENCES

Abbott LF, Dayan P (2001) Theoretical Neuroscience. Cambridge, MA: MIT Press.

Clements JD, Bekkers JM (1997) Detection of spontaneous synaptic events with an optimally scaled template. Biophys J 73:220-9.

D'Aguanno A, Bardakjian, BL, Carlen PL (1986) Passive neuronal membrane parameters: comparison of optimization and peeling methods. IEEE Trans. Biomed. Eng. 33:1188-1196.

Fucile S, Sucapan A, Eusebi F. (2005) Ca2+ permeability of nicotinic acetylcholine receptors from rat dorsal root ganglion neurones. J Physiol 565:219-28.

Gelain F, Lomander A, Vescovi AL, Zhang S (2007) Systematic studies of a self-assembling peptide nanofiber scaffold with other scaffolds. J Nanosci Nanotechnol 7:424-34.

Giugliano M, Darbon P, Arsiero M, Lüscher H-R, Streit J (2004) Single-neuron discharge properties and network activity in dissociated cultures of neocortex. J Neurophysiol 92:977–96.

Holmes WR, Segev I, Rall W (1992) Interpretation of time constant and electrotonic length estimates in multicylinder or branched neuronal structures. J Neurophysiol. 68:1401-20.

Larkum ME, Senn W, Luescher HR (2004) Top-down dendritic input increases the gain of layer 5 pyramidal neurons. Cereb Cortex 14(10):1059-70.

Lovat V, Pantarotto D, Lagostena L, Cacciari B, Grandolfo M, Righi M, Spalluto G, Prato M, Ballerini L (2005) Carbon nanotube substrates boost neuronal electrical signaling. Nano Lett 5:1107–10.

Maeda E, Robinson HP, and Kawana A (1995) The mechanisms of generation and propagation of synchronized bursting in developing networks of cortical neurons. J Neurosci 15:6834–45.

Marom S and Shahaf G (2002) Development, learning and memory in large random networks of cortical neurons: lessons beyond anatomy. Q Rev Biophys 35:63–87.

Mazzatenta A *et al*. (2007) Interfacing neurons with carbon nanotubes: electrical signal transfer and synaptic stimulation in cultured brain circuits. J. Neurosci. 27:6931-6.

Segev I (2006) What do dendrites and their synapses tell the neuron? J Neurophysiol 95:1295-7.

Tsodyks M, Pawelzik K, Markram H (1998) Neural networks with dynamic synapses. Neural Comp 10(4):821-35.

Tsodyks M, Uziel A, Markram H (2000) Synchrony generation in recurrent networks with frequency-dependent synapses. J Neurosci 20(1):RC50.